HHS Public Access

Author manuscript

J Invest Dermatol. Author manuscript; available in PMC 2016 April 01.

Published in final edited form as:

J Invest Dermatol. 2015 October ; 135(10): 2492–2501. doi:10.1038/jid.2015.166.

Protein Tyrosine Kinase 6 Regulates UVB Induced Signaling and Tumorigenesis in Mouse Skin

Michael Chastkofsky[1,2], **Wenjun Bie**, **Susan M. Ball-Kell**[3], **Yu-Ying He**[4], and **Angela L. Tyner**[1,*]

[1]Department of Biochemistry and Molecular Genetics, College of Medicine, University of Illinois at Chicago

[2]Department of Oral Sciences, College of Dentistry, University of Illinois at Chicago

[3]Global Path Imaging and Consulting, Ltd., Metamora, IL

[4]Section of Dermatology, Department of Medicine, University of Chicago

Abstract

Protein Tyrosine Kinase 6 (PTK6, also called BRK) is an intracellular tyrosine kinase expressed in the epithelial linings of the gastrointestinal tract and skin, where it is expressed in nondividing differentiated cells. We found PTK6 expression increases in the epidermis following UVB treatment. To evaluate the roles of PTK6 in the skin following UVB-induced damage, we exposed back skin of *Ptk6* +/+ and *Ptk6*−/− SENCAR mice to incremental doses of UVB for thirty weeks. Wild type mice were more sensitive to UVB and exhibited increased inflammation and greater activation of STAT3 than *Ptk6*−/− mice. Disruption of *Ptk6* did not have an impact on proliferation, although PTK6 was expressed and activated in basal epithelial cells in wild type mice following UVB treatment. However, wild type mice exhibited shortened tumor latency and increased tumor load compared with *Ptk6*−/− mice, and STAT3 activation was increased in these tumors. PTK6 activation was detected in UVB-induced tumors, and this correlated with increased activating phosphorylation of FAK and BCAR1. Activation of PTK6 was also detected in human squamous cell carcinomas of the skin. Although PTK6 plays roles in normal differentiation, it also contributes to UVB induced injury and tumorigenesis in vivo.

INTRODUCTION

Protein Tyrosine Kinase 6 (PTK6) is an intracellular tyrosine kinase that regulates growth and differentiation, as well as the response to DNA damage in epithelia [reviewed in (Brauer and Tyner, 2010)]. PTK6 was originally cloned from human melanocytes (Lee *et al*., 1993), human breast tumors (Mitchell *et al*., 1994) and the mouse intestine (Siyanova *et al*., 1994).

*Corresponding author University of Illinois College of Medicine Department of Biochemistry and Molecular Genetics M/C 669, 900 South Ashland Avenue Chicago, Illinois 60607 Phone: 312-996-7964 atyner@uic.edu.

CONFLICT OF INTEREST

The authors state no conflict of interest.”

It is most highly expressed in the gastrointestinal tract and skin, where its expression is localized to differentiated epithelial cells (Vasioukhin *et al*., 1995). PTK6 is also expressed in the prostate (Derry *et al*., 2003; Zheng *et al*., 2013a), and at low levels in human breast tissue (Peng *et al*., 2014).

PTK6 is developmentally regulated and is first expressed in the skin at mouse embryonic day 15.5, when the skin becomes stratified (Vasioukhin *et al*., 1995). PTK6 is expressed in suprabasal layers of the adult mouse and human skin (Vasioukhin *et al*., 1995; Wang *et al*., 2005). Calcium induced differentiation in embryonic mouse keratinocytes resulted in increased PTK6 activity and expression of the skin differentiation marker filaggrin (Vasioukhin and Tyner, 1997). In oral squamous cell carcinomas (SCC), PTK6 expression was reduced, and active PTK6 was excluded from the nucleus (Petro *et al*., 2004).

Analysis of *Ptk6*-null mice revealed delayed differentiation of intestinal epithelial cells (Haegebarth *et al*., 2006), and increased villus length compared with wild type intestine. PTK6 was induced in intestinal crypt cells in response to DNA-damage and *Ptk6*-null mice displayed resistance to DNA-damaged induced apoptosis in the intestine (Gierut *et al*., 2011; Haegebarth *et al*., 2009). When treated with the carcinogen azoxymethane (AOM), *Ptk6*-null mice were resistant to colon tumor formation compared with wild type mice (Gierut *et al*., 2011). Activating phosphorylation of Signal Transducer and Activator of Transcription-3 (STAT3), a substrate of PTK6 (Liu *et al*., 2006), was impaired in PTK6-null mice following administration of AOM (Gierut *et al*., 2011). STAT3 plays important roles in normal skin and skin carcinogenesis [reviewed in (Kim*et al*., 2007; Macias *et al*., 2013; Sano *et al*., 2008)]. It regulates proliferation and survival of keratinocytes following exposure to ultraviolet B radiation (UVB) and it is activated in SCC induced by UVB (Sano *et al*., 2005).

Additional PTK6 substrates include focal adhesion kinase (FAK) (Zheng *et al*., 2013a) and the adaptor protein breast cancer anti-estrogen resistance 1 (BCAR1), also commonly called p130CAS (Zheng *et al*., 2012). FAK and BCAR1 regulate cell adhesion, migration and proliferation and play important roles in cancer (Cabodi *et al*., 2010; Sulzmaier *et al*., 2014). Membrane localization of PTK6 phosphorylated on tyrosine residue 342 (PY342) has been shown to be important for activation of both FAK and BCAR1 and promotion of the epithelial mesenchymal transition (EMT) in the prostate (Zheng and Tyner, 2013).

To date, no *in vivo* studies have explored the significance of PTK6 expression in normal skin and its roles in the UVR-induced DNA-damage response and skin cancer. Using a *Ptk6*-null mouse model in the SENCAR background, we examined the impact of loss of PTK6 on skin development and examined how disruption of *Ptk6* affects UVB-induced tumor formation in mouse skin. Here we demonstrate that PTK6 is activated in both human and mouse skin tumors, and it positively regulates STAT3, FAK, and BCAR1 and contributes to UVB-induced tumor formation in vivo.

RESULTS

Disruption of *Ptk6* impairs UVB-induced tumorigenesis

PTK6 was shown to promote tumorigenesis in the mouse colon following carcinogen-induced DNA damage (Gierut *et al*., 2011). To examine the roles of PTK6 in UVB-induced carcinogenesis, we backcrossed *Ptk6*−/− C57BL/6 mice into the SENCAR mouse strain, which was previously shown to be sensitive to UVR-induced carcinogenesis (Strickland, 1982, 1986; Strickland and Swartz, 1987), and used to examine differentiation-promoting roles for PTK6 (Sik) in keratinocytes (Vasioukhin and Tyner, 1997). In order to determine the effect of PTK6 on UVB-induced tumorigenesis, shaved 8-week old wild type and *Ptk6*−/− SENCAR mice were treated with incremental doses of UVB three times each week for a total of 30 weeks. After an additional latency period of 13 weeks, mice were sacrificed at 51 weeks of age. Wild type mice began developing tumors at 28 weeks of age, and all of them had developed tumors by 36 weeks of age (Figure 1A). In contrast, *Ptk6*−/− mice did not begin to develop tumors until 32 weeks of age, and only half developed tumors. None of the control untreated wild type or *Ptk6*−/− mice, which were routinely shaved, developed tumors. Wild type mice developed a greater tumor load than *Ptk6*−/− mice, averaging 3.8 tumors/mouse, while *Ptk6*−/− mice developed an average of 1.5 tumors/mouse (Figure 1B); representative wild type and *Ptk6*−/− animals are shown at later timepoints (Figure 1C).

UVB exposure leads to increased PTK6 expression and activation in the skin

Increased sensitivity of wild type mice to UVB was observed a few weeks after beginning UVB tumor induction protocol (Figure 2A). Wild type mice experienced a moderate to severe inflammatory reaction to UVB, which was visible within a week after the first dose was administered. In comparison, *Ptk6*−/− mouse skin exhibited a mild inflammatory reaction with only a slight reddening of the skin, which faded by the second week. We examined sections of skin and detected multifocal degeneration/necrosis of the upper epidermal layers in wild type mice, sometimes with complete loss of stratum corneum. Neutrophilic migration and microabscess formation could be found in these regions with or without the intact stratum corneum in the wild type animals (Figure 2B). Little apoptosis was detected at this timepoint in wild type and *Ptk6*−/− mice by immunofluorescence for TUNEL staining (data not shown). The inflammatory reaction faded as the skin became hyperplasic and adapted to the stress of UVB treatment, completely healing after four weeks in the wild type animals.

To determine the impact of short term UVB treatment on PTK6 expression and activation, wild type SENCAR mice were treated with five doses of UVB over 10 days. PTK6 expression and activation were examined by immunoblotting and immunofluorescence. PTK6 protein expression levels increased up to three-fold (Fig. 2C and 2D), but immunoblotting was not sensitive enough to detect activation of PTK6 PY342. Using immunofluorescence, we observed hyperplasia of the skin and PTK6 was found throughout the wild type skin, with highest signals in the suprabasal layers (Figure 2E). Active PTK6 PY342 was detected a subset of cells within the basal layer. We validated the antibody against active PTK6 phosphorylated on tyrosine 342 (PY342) by using it against *Ptk6*−/− tissues, and did not detect a specific signal (control, lower right panel).

Disruption of *Ptk6* impairs STAT3 activation

STAT3 is an important regulator of inflammation [reviewed in (Yu *et al*., 2009)], and a direct substrate of PTK6. PTK6 promotes STAT3 activation by phosphorylating it on tyrosine residue 705. To examine activation of STAT3 following short-term UVB treatment, total skin lysates were probed for STAT3 activation using an antibody specific for active STAT3 PY705. STAT3 activity was not significantly different between wild type and PTK6-null untreated skin (Figure 3A). However, after short term UVB treatment, STAT3 was activated in wild type skin, but not in *Ptk6*−/− skin. Phosphorylation of STAT3 was quantitated and differences in activation between wild type and *Ptk6*−/− mice were statistically significant (p-value < 0.01) (Figure 3B). When analyzed using immunofluorescence, active STAT3 was detected in a greater number of nuclei in *Ptk6*+/+ skin than in *Ptk6*−/− skin at 10 days into the UVB-treatments (Figure 3C). At the endpoint of the long term study, we also observed an increase in STAT3 PY705 in epidermal cell nuclei of hyperplastic wild type skin compared with *Ptk6*−/− skin (Figure 3D).

PTK6 is activated in UVB-induced tumors but does not coincide with proliferation

UVB treated skin and tumors from control wild type and *Ptk6*−/− mice were examined by a veterinary pathologist (S. M. Ball-Kell). Tumors types ranged from well-differentiated SCC to spindle cell squamous cell tumors (Figure 4B, lower right panel). In both wild type and *Ptk6*−/− mice, moderate hyperkeratosis and acanthosis of the epidermis with irregular formation of rete ridges was observed. At the endpoint, which occurred either at the termination of the experiment when the mice were approximately 80 weeks of age, or when mice were sacrificed earlier at a humane, endpoint, active PY342 PTK6 was detected in the UVB irradiated skin. PTK6 PY342 was often localized to different intracellular regions within the same section in some samples. For example, while active PTK6 was detected at the membrane in the basal layer of the hyperplastic epidermis, it was in the cytoplasm or nucleus of neoplastic cells in the spindle cell squamous cell tumors (Figure 4 A, B). Hyperplasia, as well as necroulcerative dermatitis and actinic keratosis were observed in wild type mice. Total PTK6 was generally more highly expressed in the keratin 10 positive suprabasal layers of the epidermis, while active PTK6 PY342 was localized at the membrane in the more basal keratin 14 positive region of the tumors (Figure 4B). Spindle cell squamous cell tumors contained cells in the dermis that expressed both total PTK6 and PTK6 PY342 (Figure 4B). Immunohistochemistry for keratin-10 and keratin-14 expression confirmed the epithelial origin of the tumor cells within the dermis (Figure 4B).

To determine the roles of PTK6 in regulating proliferation at the endpoint of the experiment, BrdU incorporation was examined in hyperplastic skin, spindle cell squamous cell tumors (Fig. 4C) and SCC from UVB-treated *Ptk6*+/+ and *Ptk6*−/− mice. No significant differences in the numbers of BrdU incorporating S-phase cells were detected in any of the samples. Costaining for active PTK6 PY342 and BrdU incorporation indicated that cells with active PTK6 at the membrane are distinct from the BrdU incorporating cells, suggesting the active PTK6 does not directly promote S-phase progression at the time points examined. We also did not detect a significant difference in BrdU incorporation in younger *Ptk6*+/+ and *Ptk6*−/− mouse skin after 10 days of UVB treatment (not shown).

PTK6 regulates phosphorylation of FAK and BCAR1 in UVB-treated skin

PTK6 mediated tyrosine phosphorylation of FAK has previously been shown to inhibit anoikis (Zheng *et al*., 2013a). PTK6 regulates phosphorylation of FAK at several tyrosine residues, including Y576/Y577 and Y925 which regulate activation and GRB2 binding respectively (Sulzmaier *et al*., 2014). To examine PTK6-mediated regulation of FAK, we stained sections of skin with antibodies specific for FAK phosphorylated on Y576/Y577 and Y925. No differences in phosphorylation of Y576/577 or Y925 were observed between wild type and *Ptk6*−/− untreated skin (Figure 5A). After short-term (10 day) UVB-treatment, some wild type epidermal cells contained FAK phosphorylated at both Y576/Y577 and at Y925, while no specific signals could be detected in *Ptk6*−/−epidermis (Figure 5B). At the endpoint, FAK phosphorylation at Y576/Y577 and Y925 was detected throughout the *Ptk6*+/+ hyperplastic epidermis, with striking membrane localization of PY925 in the upper layers. The pattern of FAK phosphorylation was less intense and much less striking in the *Ptk6*−/− skin (Figure 5C).

We previously showed that PTK6 promotes phosphorylation of tyrosine residue 165 in BCAR1 (p130CAS) (Zheng *et al*., 2012). In untreated skin, cells strongly positive for BCAR1 phosphorylated on tyrosine residue 165 (Y165) were detected only in *Ptk6*+/+ skin, but not in *Ptk6*−/− skin (Figure 5D, arrows). UVB irradiation promotes Y165 phosphorylation of BCAR1 in both genotypes, but the BCAR1 PY165 signal is stronger in *Ptk6*+/+ skin than in *Ptk6*−/− skin (Figure 5E). BCAR1 is strongly phosphorylated at Y165 in the endpoint *Ptk6*+/+ skin, particularly in the suprabasal layers of the epidermis, but is not highly phosphorylated in *Ptk6*−/− skin (Figure 5F).

PTK6 is activated in human cutaneous SCC

In order to explore the possible clinical significance of our mouse data, we examined PTK6 expression in a set of 34 human biopsy sections that included normal skin and SCC. Sections were double stained for total and active PTK6 (PY342), and a section from the same block was H & E stained (Figure 6). In normal human skin, PTK6 expression was detected in the suprabasal layer of the epidermis, with minimal expression in the basal layer (Figure 6A), as reported previously (Vasioukhin *et al*., 1995; Wang *et al*., 2005). Significant activating phosphorylation of PTK6 (PY342) was not detected in normal human skin. However, in SCC, PTK6 is activated and phosphorylated in some epidermal cells, particularly those located at the borders of the epidermis/dermis (SCC1A, 1B). In another SSC sample (SCC #2), most active PTK6 PY342 was found adjacent to the keratinized surface area and next to a blood vessel (Figure 6A). These data show that high PTK6 expression levels do not always correlate with PTK6 activation. In addition, activation of PTK6 is regulated by environmental cues and is not uniformly detected in PTK6 positive tissue.

Transcriptome profiling of human cutaneous SCC at different stages of progression was recently performed by Lambert and colleagues using laser capture microdissection and microarray analysis (Lambert *et al*., 2014). By analyzing PTK6 mRNA levels in the Lambert datasets, we found that *Ptk6* transcript levels were reduced in SCC compared with the precancerous actinic keratosis (Figure 6B). In addition, there was a significant difference

in PTK6 transcript levels between well-differentiated SCC and poorly-differentiated SCC. While PTK6 protein expression levels did not appear reduced in SCC examined by immunofluorescence, this is not a highly quantitative technique. It is also possible that posttranscriptional mechanisms are important for regulation of PTK6 protein levels.

DISCUSSION

PTK6 belongs to a small family of intracellular tyrosine kinases that includes FRK and SRMS, and is evolutionarily related to the SRC-family (D'Aniello *et al*., 2008; Serfas and Tyner, 2003). Although PTK6-family kinases share structural similarity with SRC-family kinases, PTK6 family members lack an amino terminal SH4 domain that promotes lipid modification and membrane targeting. Nevertheless, membrane association of active endogenous PTK6 has been detected in mouse and human prostate (Zheng *et al*., 2013a; Zheng and Tyner, 2013) and mammary gland (Peng *et al*., 2013; Peng *et al*., 2014) tumors. A variety of data suggest that the intracellular localization and activation of PTK6 has profound effects on its activities. PTK6 can be detected in nuclei of normal differentiated glands of the human prostate, but nuclear localization is lost in prostate cancer (Derry *et al*., 2003). Reintroduction of ectopic PTK6 into the nuclei of prostate cancer cells is growth inhibiting (Brauer *et al*., 2010). In studies where PTK6 was targeted to the plasma membrane in cell lines by the addition of a SH4 domain, membrane association of active PTK6 was sufficient to transform mouse embryonic fibroblasts (Zheng *et al*., 2013a), promote the epithelial mesenchymal transition, and contribute to human xenograft prostate tumor growth in vivo (Zheng *et al*., 2013b).

Here, we demonstrate that active PTK6 is associated with the plasma membrane in mouse skin tumors induced by UVB and in human cutaneous SCC. Since PTK6 is expressed in normal differentiated nondividing epithelial cells in the gastrointestinal tract and skin (Vasioukhin *et al*., 1995), and has been shown to promote differentiation in small intestine (Haegebarth *et al*., 2006) and cultured keratinocytes (Vasioukhin and Tyner, 1997; Wang *et al*., 2005), we initially proposed that PTK6 might have tumor suppressor functions in the gut and skin. However, we found that *Ptk6* impairs cutaneous tumor growth in the UVB skin model, demonstrating PTK6 signaling is contributing to tumor development in vivo. These data are consistent with those obtained with intestinal tissues where PTK6 is also normally expressed in the nondividing, differentiated epithelial cells. Disruption of the *Ptk6* gene led to significantly reduced tumor formation in mice treated with the colon carcinogen AOM, and impaired activation of STAT3 (Gierut *et al*., 2011).

In the colon, disruption of *Ptk6* impaired activation of STAT3, a transcription factor that promotes epithelial tumor initiation and progression (Gierut *et al*., 2011). In this study, we observed increased activating tyrosine phosphorylation and nuclear localization of STAT3 in wild type UV-irradiated skin treated with both the short-term and long-term UVB protocols and in tumors of wild type mice compared with *Ptk6* −/−mice (Fig. 3). STAT3 activation is positively regulated by tyrosine phosphorylation of tyrosine residue 705, which is a target of PTK6 (Liu *et al*., 2006). Several studies have demonstrated roles for STAT3 in skin tumorigenesis [reviewed in (Macias *et al*., 2013; Sano *et al*., 2008)]. STAT3-null mice were resistant to tumorigenesis induced by a 7,12-dimethylbenz[a]anthracene (DMBA/ 12-

O-tetradecanoylphorbol-13-acetate (TPA) protocol (Chan *et al*., 2004). Consistently, disruption of STAT3 impaired and overexpression of STAT3 promoted UVB-induced skin carcinogenesis in mouse models (Kim *et al*., 2009).

Interestingly, membrane association of active PTK6 in established tumors did not correlate with proliferation (Figure 4C), and we were unable to detect significant differences in proliferation in skin between wild type and *Ptk6*−/− mice at any of the timepoints examined. In previous studies, we also found no correlation between PTK6 activation and proliferation in established mouse tumors in the prostate (Zheng *et al*., 2013b) or mammary gland (Peng and Tyner, in preparation). However, induction of PTK6 in the mammary glands of *Ptk6*+/+ ERBB2 overexpressing mice prior to tumor formation or significant hyperplasia correlated with increased epithelial cell proliferation and STAT3 activation compared with the *Ptk6*−/− mammary gland (Peng and Tyner, in preparation). Lack of PTK6 mediated activation of STAT3 could at least in part explain our finding that disruption of PTK6 impairs UVB-induced tumorigenesis in the mouse.

Reduced tyrosine phosphorylation of the PTK6 substrates FAK (Zheng *et al*., 2013a) and BCAR1 (Zheng *et al*., 2012) was detected in *Ptk6*−/− mice compared with wild type controls (Fig. 5). While BCAR1 is a substrate of FAK, PTK6 can directly phosphorylate both of these proteins (Zheng and Tyner, 2013). Both FAK and BCAR1 function in regulating cell adhesion, migration, and the cell cycle [reviewed in (Barrett *et al*., 2013; Duperret and Ridky, 2013; Sulzmaier *et al*., 2014)]. Disruption of FAK in keratinocytes led to some proliferation defects and a thinner epidermis (Essayem *et al*., 2006). FAK can regulate SCC cell survival (Zhang *et al*., 2004), and has been shown to play roles in cutaneous cancer stem cells (Schober and Fuchs, 2011). BCAR1 plays an important role in several oncogenic signaling pathways including the ERBB2 pathway (Cabodi *et al*., 2010; Cabodi *et al*., 2006).

While an intact *Ptk6* gene enhanced UVB-induced tumorigenesis in SENCAR mice, our analysis of microarray data of mRNA expression in human SCC (Lambert *et al*., 2014) suggested that PTK6 mRNA expression levels decrease in less differentiated human cutaneous tumors. This correlates with the expression pattern observed in normal mouse and human skin, where PTK6 is expressed in the differentiated nondividing layers of the epidermis. A number of studies suggest that PTK6 has context specific functions and its roles differ depending on cell type/tissue, activation, and intracellular localization (Brauer *et al*., 2010; Derry *et al*., 2003; Peng *et al*., 2014; Zheng and Tyner, 2013). Activation of PTK6 at the plasma membrane, as reported here in mouse and human skin tumors, may be a primary requirement for its tumor-promoting functions. Understanding the significance of changes in the intracellular localization and activation of PTK6 will be critical for determining when PTK6 may be an effective therapeutic target in cancer.

MATERIALS AND METHODS

Mouse Experiments

SENCAR (SENsitive to CARcinogenesis) mice were generated by crossing Charles River CD1 mice with skin tumor-sensitive mice (STS) mice, and they are hypersensitive to UVR

(Strickland, 1982; Strickland and Swartz, 1987). This strain has previously been used as a source of primary keratinocytes for the study of activation of PTK6 (Vasioukhin and Tyner, 1997) and other tyrosine kinases (Calautti *et al*., 1995). The *Ptk6*-null mouse model (B6.129SV-*Ptk6*^{tm1Aty}) in C57BL/6 was backcrossed for over 10 generations to generate a SENCAR *Ptk6*−/− mouse model. Age and sex matched were used for all experiments. All mouse experiments were reviewed and approved by the University of Illinois at Chicago Animal Care Committee.

For UVB treatment, the backs of 8 week-old male adult mice were shaved 24 hours prior to treatment. Mice were irradiated using an FB-UVXL-1000 UV crosslinker (Spectroline) fitted with five 8-Watt 312 nm tubes (Spectronics BLE-8T312, with filter assembly). The dorsal epidermis was exposed to 220 mJ/cm^2 UVB irradiation three times per week for weeks 1-6, 260 mJ/cm^2 UVB for weeks 7-8, 300 mJ/cm^2 UVB for weeks 9-10, 360 mJ/cm^2 UVB for weeks 11-12, 405 mJ/cm^2 UVB for weeks 13-14 and 450 mJ/cm^2 UVB for weeks 15-30. To achieve 220-450 mJ/cm^2 UVB irradiation mice were irradiated for 3-6.5 minutes. UVB irradiation was stopped at 30 weeks and mice were kept without further treatment for 43 weeks. Control animals were regularly shaved, but not exposed to UVB. Mice were photographed and weighed prior to each UV treatment. Short-term UVB treatments consisted of five doses of 220 mJ/cm^2 UVB five times over the course of 10 days. The mice were sacrificed after 43 weeks and their skin harvested. The mice were injected intraperitoneally with BrdU (100 μg/g body weight) in PBS 2 hours before sacrifice to measure proliferation.

Antibodies

Anti-mouse PTK6 (C17), FAK (C20), and Cytokeratin 14 were purchased from Santa Cruz Biotechnology (Santa Cruz, CA). Antibodies against STAT3, P-STAT3 (Y705), P-FAK (Y576,Y577), P-BCAR1 (Y165), and GAPDH (14C10) were purchased from Cell Signaling Technology (Danvers, MA). The anti-BCAR1 antibody came from BD Pharmingen. The P-PTK6 (Y342) antibody came from Millipore. Cytokeratin 10 antibody was purchased from Abcam (Cambridge, MA). Donkey anti-rabbit and sheep anti-mouse antibodies conjugated to horseradish peroxidase were used as secondary antibodies for immunoblotting (Amersham Biosciences) and were detected by chemiluminescence using SuperSignal West Dura extended duration substrate (Pierce).

Protein Lysates

Skin tissue was homogenized in 1% Triton X-100 lysis buffer (1% Triton X-100, 20 mM HEPES, pH 7.4, 150 mM NaCl, 1 mM EDTA, 1 mM EGTA, 10 mM sodium pyrophosphate, 100 mM NaF, 5 mM iodoacetic acid, 0.2 mM phenylmethylsulfonyl fluoride (PMSF), protease inhibitor mixture (Roche Applied Science). Samples were separated by SDS-PAGE and transferred to Immobilon-P membrane (Millipore) for immunoblotting.

Histology and Immunofluorescence

Skin tissue was harvested and fixed in 10% neutral-buffered formalin, embedded in paraffin blocks, and cut into 5 micron sections. The slides were stained with hematoxylin and eosin (H & E) prior to histopathologic examination. For immunofluorescence microscopy, the

slides were deparaffinized by xylenes, dehydrated with ethanol, and rehydrated in PBS. Antigen retrieval was performed by incubation in 0.01 M citrate buffer (pH 6.0) at 75°C for 20 minutes. Sections were blocked in TNT for 30 minutes at room temperature. The primary antibody was incubated overnight at 4°C in blocking buffer and washed in TNT, followed by the secondary incubation with biotinylated anti-rabbit or anti-mouse secondary antibodies at room temperature for 30 minutes. Sections were then stained with fluorescein isothiocyanate (FITC)-conjugated avidin (Vector Laboratories, Burlingame, CA). For double staining, FITC-conjugated anti-mouse secondary antibodies (Sigma-Aldrich) were used to detect primary antibodies made in mouse (green), and biotinylated anti-rabbit secondary antibodies (Vector Laboratories) were used and then incubated with Alexa Fluor 594 strepavidin conjugate (Life Technologies) to detect primary antibodies made in rabbit (red). Slides were mounted in Vectashield fluorescent mounting medium containing 4',6-diamidino-2-phenylindole (DAPI) (Vector Laboratories). The skin was then viewed using standard UV, rhodamine, or FITC filters under 20X and 40X differential interference contrast objectives using a Zeiss LSM 5 PASCAL confocal microscope. Images were taken using an Axiocam HRc color digital camera and LSM 5 PASCAL software (Zeiss, Jena, Germany).

Human Tissues

Human tissue sections diagnosed as SCC were obtained from the tissue bank in the Section of Dermatology (Department of Medicine, University of Chicago, Chicago IL) and their use was approved by the University of Chicago Institutional Review Board. Slides were stained with H&E, total PTK6 (G6 antibody), and PY342PTK6 antibodies.

Statistical Analyses

Quantitative analysis of immunoblot data was performed using the NIH ImageJ program. For all statistical studies, p-values were determined using a two-tailed Student's t-test (Microsoft Excel 2011). Statistical significance was determined by a p-value that was less than 0.05.

ACKNOWLEDGEMENTS

A.L.T. is supported by National Institutes of Health Grant DK44525 (A.L.T.). M.C received support from an NRSA/NIH Institutional T32 training grant, the Multidisciplinary Oral Science Training grant; 5-T32-DE-18381-4. We thank Dr. Hui Xie, Ms. Priya Mathur, and Mr. Darren Wozniak (University of Illinois at Chicago) for helpful discussions and comments.

REFERENCES

Barrett A, Pellet-Many C, Zachary IC, et al. p130Cas: a key signalling node in health and disease. Cellular Signalling. 2013; 25:766–77. [PubMed: 23277200]

Brauer PM, Tyner AL. Building a better understanding of the intracellular tyrosine kinase PTK6 - BRK by BRK. Biochimica et Biophysica Acta. 2010; 1806:66–73. [PubMed: 20193745]

Brauer PM, Zheng Y, Wang L, et al. Cytoplasmic retention of protein tyrosine kinase 6 promotes growth of prostate tumor cells. Cell Cycle. 2010; 9:4190–9. [PubMed: 20953141]

Cabodi S, del Pilar Camacho-Leal M, Di Stefano P, et al. Integrin signalling adaptors: not only figurants in the cancer story. Nature Reviews Cancer. 2010; 10:858–70. [PubMed: 21102636]

Cabodi S, Tinnirello A, Di Stefano P, et al. p130Cas as a new regulator of mammary epithelial cell proliferation, survival, and HER2-neu oncogene-dependent breast tumorigenesis. Cancer Research. 2006; 66:4672–80. [PubMed: 16651418]

Calautti E, Missero C, Stein PL, et al. fyn tyrosine kinase is involved in keratinocyte differentiation control. Genes & Development. 1995; 9:2279–91. [PubMed: 7557381]

Chan KS, Sano S, Kiguchi K, et al. Disruption of Stat3 reveals a critical role in both the initiation and the promotion stages of epithelial carcinogenesis. The Journal of Clinical Investigation. 2004; 114:720–8. [PubMed: 15343391]

D'Aniello S, Irimia M, Maeso I, et al. Gene expansion and retention leads to a diverse tyrosine kinase superfamily in amphioxus. Molecular Biology and Evolution. 2008; 25:1841–54. [PubMed: 18550616]

Derry JJ, Prins GS, Ray V, et al. Altered localization and activity of the intracellular tyrosine kinase BRK/Sik in prostate tumor cells. Oncogene. 2003; 22:4212–20. [PubMed: 12833144]

Duperret EK, Ridky TW. Focal adhesion complex proteins in epidermis and squamous cell carcinoma. Cell cycle. 2013; 12:3272–85. [PubMed: 24036537]

Essayem S, Kovacic-Milivojevic B, Baumbusch C, et al. Hair cycle and wound healing in mice with a keratinocyte-restricted deletion of FAK. Oncogene. 2006; 25:1081–9. [PubMed: 16247468]

Gierut J, Zheng Y, Bie W, et al. Disruption of the Mouse Protein Tyrosine Kinase 6 Gene Prevents STAT3 Activation and Confers Resistance to Azoxymethane. Gastroenterology. 2011; 141:1371–80. e2. [PubMed: 21741923]

Haegebarth A, Bie W, Yang R, et al. Protein tyrosine kinase 6 negatively regulates growth and promotes enterocyte differentiation in the small intestine. Molecular and Cellular Biology. 2006; 26:4949–57. [PubMed: 16782882]

Haegebarth A, Perekatt AO, Bie W, et al. Induction of protein tyrosine kinase 6 in mouse intestinal crypt epithelial cells promotes DNA damage-induced apoptosis. Gastroenterology. 2009; 137:945–54. [PubMed: 19501589]

Kim DJ, Angel JM, Sano S, et al. Constitutive activation and targeted disruption of signal transducer and activator of transcription 3 (Stat3) in mouse epidermis reveal its critical role in UVB-induced skin carcinogenesis. Oncogene. 2009; 28:950–60. [PubMed: 19137019]

Kim DJ, Chan KS, Sano S, et al. Signal transducer and activator of transcription 3 (Stat3) in epithelial carcinogenesis. Mol Carcinog. 2007; 46:725–31. [PubMed: 17610223]

Lambert SR, Mladkova N, Gulati A, et al. Key differences identified between actinic keratosis and cutaneous squamous cell carcinoma by transcriptome profiling. British journal of cancer. 2014; 110:520–9. [PubMed: 24335922]

Lee ST, Strunk KM, Spritz RA. A survey of protein tyrosine kinase mRNAs expressed in normal human melanocytes. Oncogene. 1993; 8:3403–10. [PubMed: 8247543]

Liu L, Gao Y, Qiu H, et al. Identification of STAT3 as a specific substrate of breast tumor kinase. Oncogene. 2006; 25:4904–12. [PubMed: 16568091]

Macias E, Rao D, Digiovanni J. Role of stat3 in skin carcinogenesis: insights gained from relevant mouse models. J Skin Cancer. 2013; 2013:684050. [PubMed: 23577258]

Mitchell PJ, Barker KT, Martindale JE, et al. Cloning and characterisation of cDNAs encoding a novel non-receptor tyrosine kinase, brk, expressed in human breast tumours. Oncogene. 1994; 9:2383–90. [PubMed: 8036022]

Peng M, Ball-Kell SM, Franks RR, et al. Protein tyrosine kinase 6 regulates mammary gland tumorigenesis in mouse models. Oncogenesis. 2013; 2:e81. [PubMed: 24323291]

Peng M, Emmadi R, Wang Z, et al. PTK6/BRK is expressed in the normal mammary gland and activated at the plasma membrane in breast tumors. Oncotarget. 2014; 5:6038–48. [PubMed: 25153721]

Petro BJ, Tan RC, Tyner AL, et al. Differential expression of the non-receptor tyrosine kinase BRK in oral squamous cell carcinoma and normal oral epithelium. Oral Oncol. 2004; 40:1040–7. [PubMed: 15509496]

Rasband, WS. ImageJ. U S National Institutes of Health; Bethesda, Maryland, USA: 2011. http://imagej.nih.gov/ij/

Sano S, Chan KS, DiGiovanni J. Impact of Stat3 activation upon skin biology: a dichotomy of its role between homeostasis and diseases. J Dermatol Sci. 2008; 50:1–14. [PubMed: 17601706]

Sano S, Chan KS, Kira M, et al. Signal transducer and activator of transcription 3 is a key regulator of keratinocyte survival and proliferation following UV irradiation. Cancer Res. 2005; 65:5720–9. [PubMed: 15994947]

Schober M, Fuchs E. Tumor-initiating stem cells of squamous cell carcinomas and their control by TGF-beta and integrin/focal adhesion kinase (FAK) signaling. Proceedings of the National Academy of Sciences of the United States of America. 2011; 108:10544–9. [PubMed: 21670270]

Serfas MS, Tyner AL. Brk, Srm, Frk, and Src42A form a distinct family of intracellular Src-like tyrosine kinases. Oncol Res. 2003; 13:409–19. [PubMed: 12725532]

Siyanova EY, Serfas MS, Mazo IA, et al. Tyrosine kinase gene expression in the mouse small intestine. Oncogene. 1994; 9:2053–7. [PubMed: 8208550]

Strickland PT. Tumor induction in Sencar mice in response to ultraviolet radiation. Carcinogenesis. 1982; 3:1487–9. [PubMed: 7151263]

Strickland PT. Photocarcinogenesis and persistent hyperplasia in UV-irradiated SENCAR mouse skin. Environmental health perspectives. 1986; 68:131–4. [PubMed: 3780624]

Strickland PT, Swartz RP. Inheritance of susceptibility to phototumorigenesis and persistent hyperplasia in F1 hybrids between SENCAR mice and BALB/c or C57BL/6 mice. Cancer Research. 1987; 47:6294–6. [PubMed: 3677078]

Sulzmaier FJ, Jean C, Schlaepfer DD. FAK in cancer: mechanistic findings and clinical applications. Nature Reviews Cancer. 2014; 14:598–610. [PubMed: 25098269]

Vasioukhin V, Serfas MS, Siyanova EY, et al. A novel intracellular epithelial cell tyrosine kinase is expressed in the skin and gastrointestinal tract. Oncogene. 1995; 10:349–57. [PubMed: 7838533]

Vasioukhin V, Tyner AL. A role for the epithelial-cell-specific tyrosine kinase Sik during keratinocyte differentiation. Proc Natl Acad Sci U S A. 1997; 94:14477–82. [PubMed: 9405638]

Wang TC, Jee SH, Tsai TF, et al. Role of breast tumour kinase in the in vitro differentiation of HaCaT cells. Br J Dermatol. 2005; 153:282–9. [PubMed: 16086737]

Yu H, Pardoll D, Jove R. STATs in cancer inflammation and immunity: a leading role for STAT3. Nat Rev Cancer. 2009; 9:798–809. [PubMed: 19851315]

Zhang Y, Lu H, Dazin P, et al. Squamous cell carcinoma cell aggregates escape suspension-induced, p53-mediated anoikis: fibronectin and integrin alphav mediate survival signals through focal adhesion kinase. The Journal of Biological Chemistry. 2004; 279:48342–9. [PubMed: 15331608]

Zheng Y, Asara JM, Tyner AL. Protein-tyrosine Kinase 6 Promotes Peripheral Adhesion Complex Formation and Cell Migration by Phosphorylating p130 CRK-associated Substrate. The Journal of Biological Chemistry. 2012; 287:148–58. [PubMed: 22084245]

Zheng Y, Gierut J, Wang Z, et al. Protein tyrosine kinase 6 protects cells from anoikis by directly phosphorylating focal adhesion kinase and activating AKT. Oncogene. 2013a; 32:4304–12. [PubMed: 23027128]

Zheng Y, Tyner AL. Context-specific protein tyrosine kinase 6 (PTK6) signalling in prostate cancer. Eur J Clin Invest. 2013; 43:397–404. [PubMed: 23398121]

Zheng Y, Wang Z, Bie W, et al. PTK6 activation at the membrane regulates epithelial-mesenchymal transition in prostate cancer. Cancer Research. 2013b; 73:5426–37. [PubMed: 23856248]

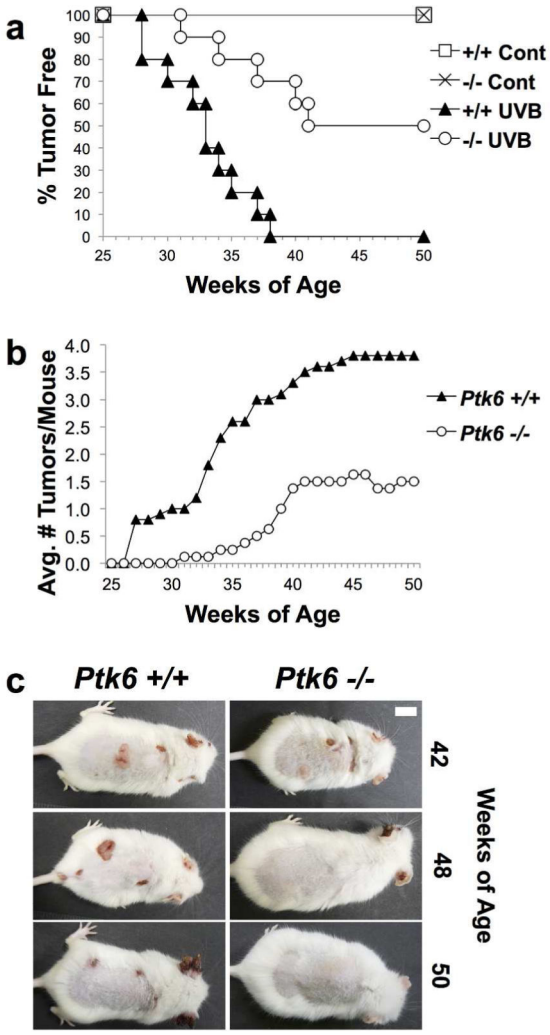

Figure 1. Ptk6−/− mice are resistant to UVB induced tumorigenesis

A: Kinetics of UVB-induced tumor development in wild type and *Ptk6*−/− mouse skin. *Ptk6*+/+ mice developed tumors sooner than *Ptk6*−/− mice. All *Ptk6*+/+ mice developed tumors, while only half of *Ptk6*−/− mice did. **B:** The average number of tumors that developed in wild type and *Ptk6*−/− mice is shown. **C:** Tumor formation in representative wild type and *Ptk6*−/− animals is shown at the indicated timepoints, including one of the tumor positive *Ptk6*−/− mice at 42 weeks.

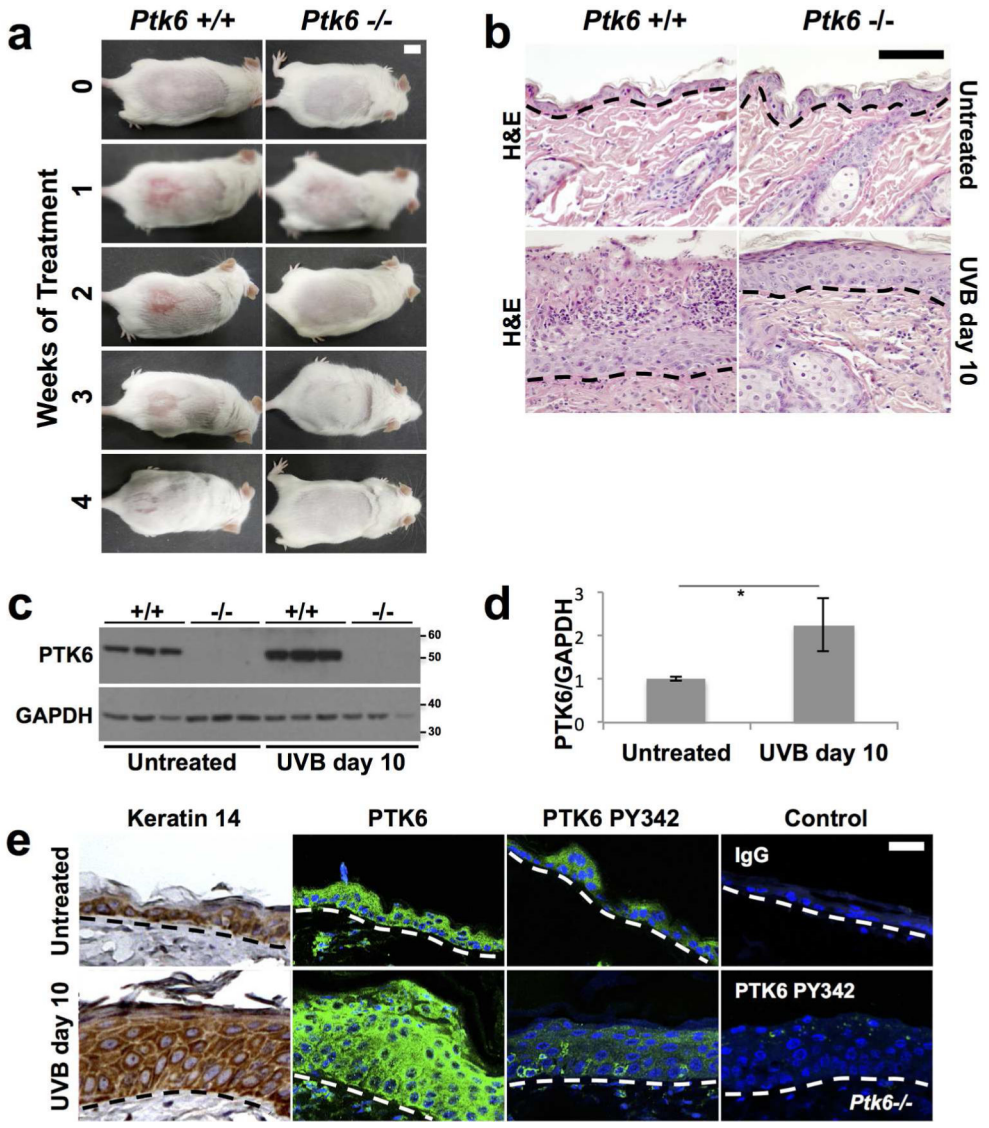

Figure 2. Increased Inflammation and PTK6 expression are detected in wild type mice after UVB treatment

A: Increased and prolonged inflammation was detected in wild type mice compared with *Ptk6*−/− mice after short term exposure to UVB. *Ptk6*+/+ mice (left panels) developed erythema and an inflammatory reaction on the lower dorsal skin within a week after beginning UVB treatments. Mice were treated with UVB three times a week. Size bar = 1 cm. **B:** Increased degeneration and necrosis of the upper epidermal layers with neutrophilic migration and microabscess formation was detected in wild type mice when compared with *Ptk6*−/− skin at 10 days post initiation of short term UVB treatment. Representative H & E stained sections are shown. **C:** PTK6 expression is induced by UVB treatment in mouse skin. Lysates of adult (8-weeks old) mouse skin after short-term UVB were prepared and analyzed by immunoblotting. Each lane represents a sample from a different mouse. GAPDH was used as a loading control. **D:** The increase in PTK6 expression after UVB treatment (2C) was quantified using ImageJ (Rasband, 2011). The intensity of PTK6 signal was normalized to intensity of the GAPDH loading control and averaged across all samples.

p-value = 0.025. **E:** Total PTK6 and active PTK6 Y342 expression was examined by immunofluorescence in untreated and UVB-treated skin. Keratin 14 is expressed throughout the hyperplastic skin after UVB treatment. Controls included staining with IgG and staining of UVB-treated *Ptk6*−/− skin with the antibody against PTK6 PY342. No specific signal for PY342 was detected in *Ptk6*−/− mice. Size bar = 20 μm.

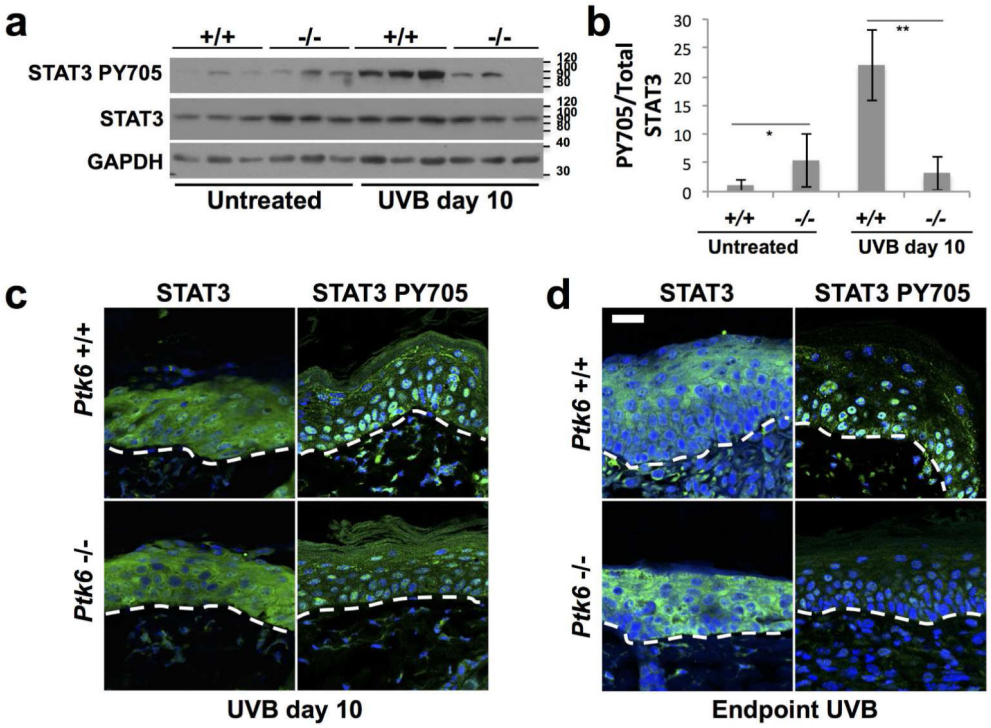

Figure 3. PTK6 promotes STAT3 activation after UVB treatment

A: Increased STAT3 PY705 was detected in skin tissue lysates from wild type UVB-treated mouse skin compared with in *Ptk6*−/− UVB-treated mouse skin. Each lane represents lysate from an individual mouse, and a minimum of three mice were examined per treatment. **B:** Changes in STAT3 activation (PY705) after UVB treatment were quantified using ImageJ (Rasband, 2011). Relative levels of PY705 STAT3 normalized to total STAT3 were averaged across all samples. No significant difference between PY705 levels was detected in the untreated *Ptk6*+/+ and *Ptk6*−/− skin (p-value = 0.19), but there is a significant difference between PY705 STAT3 levels in *Ptk6*+/+ and *Ptk6*−/− UVB-treated skin (p-value = 0.009). **C:** Increased nuclear localization of STAT3 PY705 was detected by immunofluorescence in wild type mouse skin (10 day UVB treatment). **D:** Increased nuclear localization of STAT3 PY705 was detected by immunofluorescence in wild type mouse skin following long-term UVB treatment (experiment endpoint). Size bar = 20 μm.

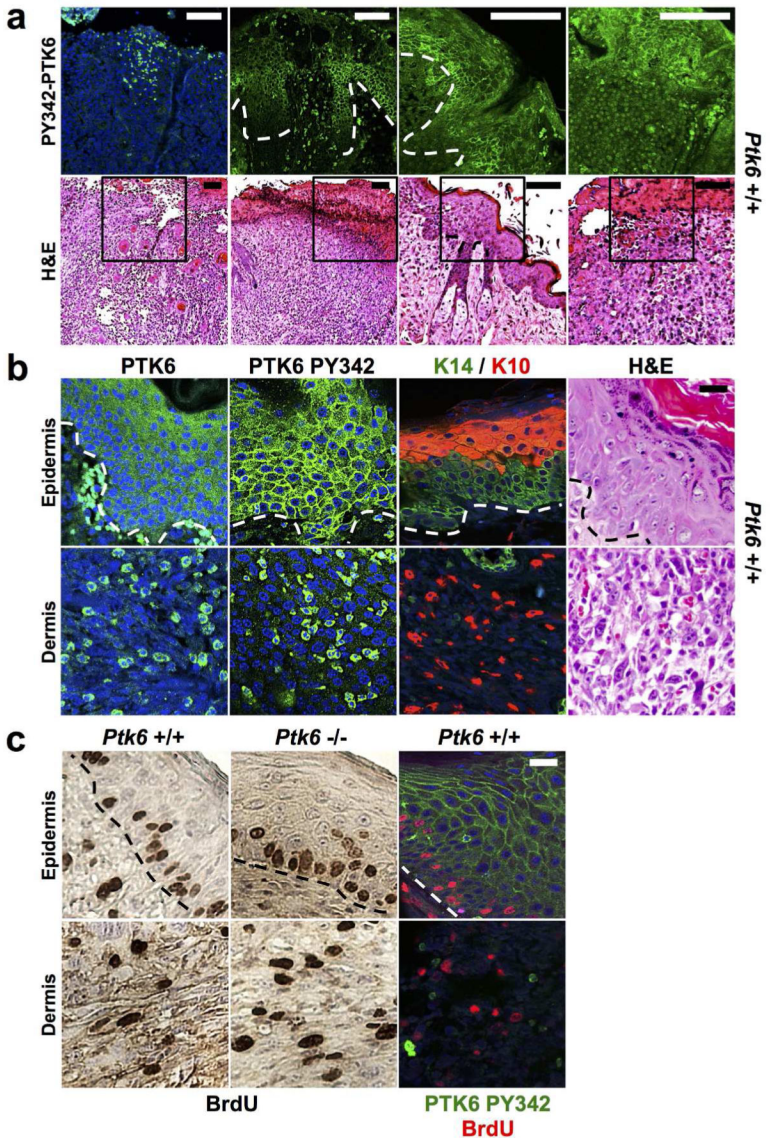

Figure 4. PTK6 is activated in UVB damaged skin and UVB-induced skin tumors

A: PTK6 activation in different cellular locations following long-term UVB treatment. PTK6 PY342 localizes to the cytoplasm in neoplastic cells infiltrating the dermis (left panel). Active PTK6 PY342 is associated with the plasma membrane in the epidermal cell layers (center panels). Membrane and nuclear localization of PTK6 PY342 can be detected in different regions of the same section in endpoint UVB-treated hyperplastic skin showing epidermal necrosis and dermal inflammation (right panel). Size bar = 100 μm. **B:** Differential localization of active PTK6 in epidermal cells and neoplastic cells in the dermis of spindle cell squamous cell tumors. Tumors that formed in wild type mice were incubated with antibodies against total PTK6 and active PTK6 PY342. In actinic keratosis and anaplastic spindle cell tumors, total PTK6 is expressed throughout the adjacent or overlying epidermis, and PTK6 PY342 is present at the plasma membrane. Both total PTK6 and PTK6 PY342 are found in the cytoplasm of keratin-expressing cells of epithelial origin in the dermis. Keratin 14 expression was detected in suprabasal layers of the hyperplastic skin.

Infiltrative neoplastic cells expressed either keratin 14 or keratin 10 identifying them as epithelial in origin. Size bar = 20 μm. **C:** BrdU incorporation does not correlate with activation of PTK6. BrdU incorporation (red) and membrane associated PTK6 PY342 (FITC, green) does not colocalize in hyperplastic skin or spindle cell squamous cell tumors. Size bar = 20 μm.

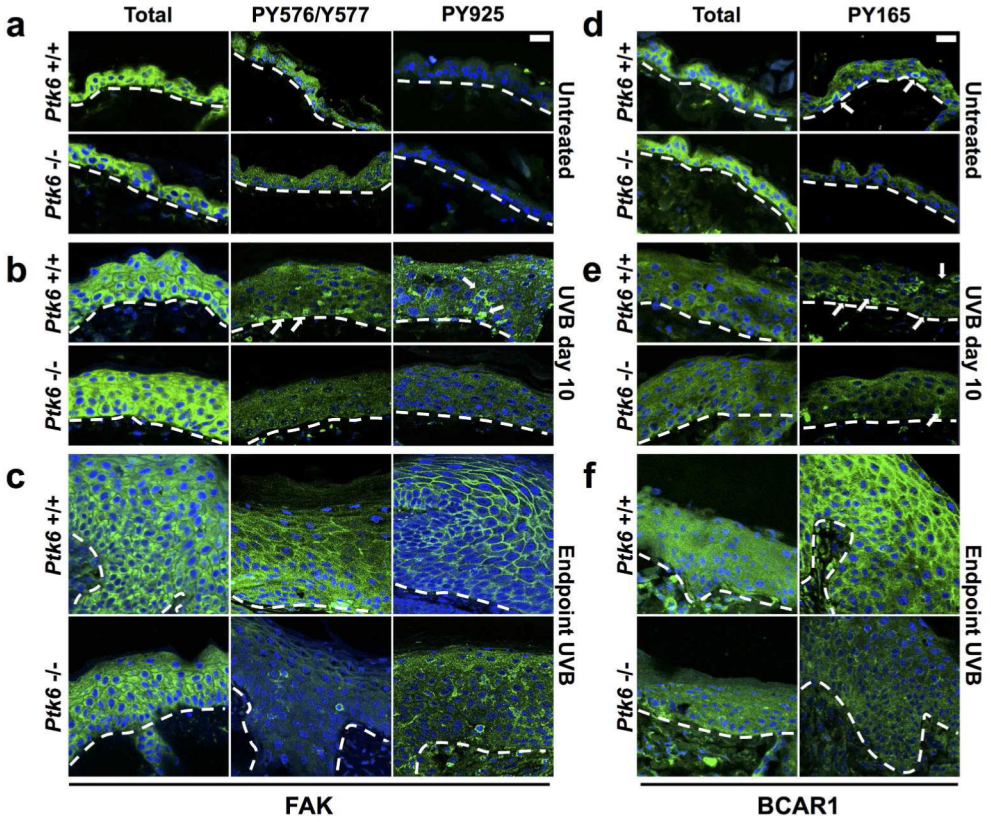

Figure 5. Activation of FAK and BCAR1 in UVB-treated SENCAR Mouse Skin

A: FAK is expressed throughout the epidermis in adult mouse skin, but is not phosphorylated in either *Ptk6*+/+ or *Ptk6*−/− adult mouse skin. **B:** After 10 days of regular UVB treatment, FAK becomes phosphorylated at the membrane in *Ptk6*+/+ adult mouse skin at both phosphorylation sites. There is no phosphorylation of FAK at either site in *Ptk6*−/− mouse skin. **C:** FAK is phosphorylated at both Y576/Y577 and at Y925 at the membrane in both *Ptk6*+/+ and *Ptk6*−/− mouse skin tumors, but is much more pervasive in *Ptk6*+/+ mouse skin tumors. **D:** BCAR1 is expressed throughout the epidermis in adult mouse skin. BCAR1 is phosphorylated in the basal layer of *Ptk6*+/+ mouse skin. There is no phosphorylation of BCAR1 in *Ptk6*−/− mouse skin. **E:** Within 10 days of regular UVB treatment, BCAR1 phosphorylation increases in both genotypes. Phosphorylation of BCAR1 remains higher in *Ptk6*+/+ mouse skin than in *Ptk6*−/− mouse skin. **F:** BCAR1 is phosphorylated in both *Ptk6*+/+ and *Ptk6*−/− mouse skin tumors, but is much more pervasive in *Ptk6*+/+ mouse skin tumors. Size bar = 20 μm. Dashed lines indicate the boundary between epidermis and dermis.

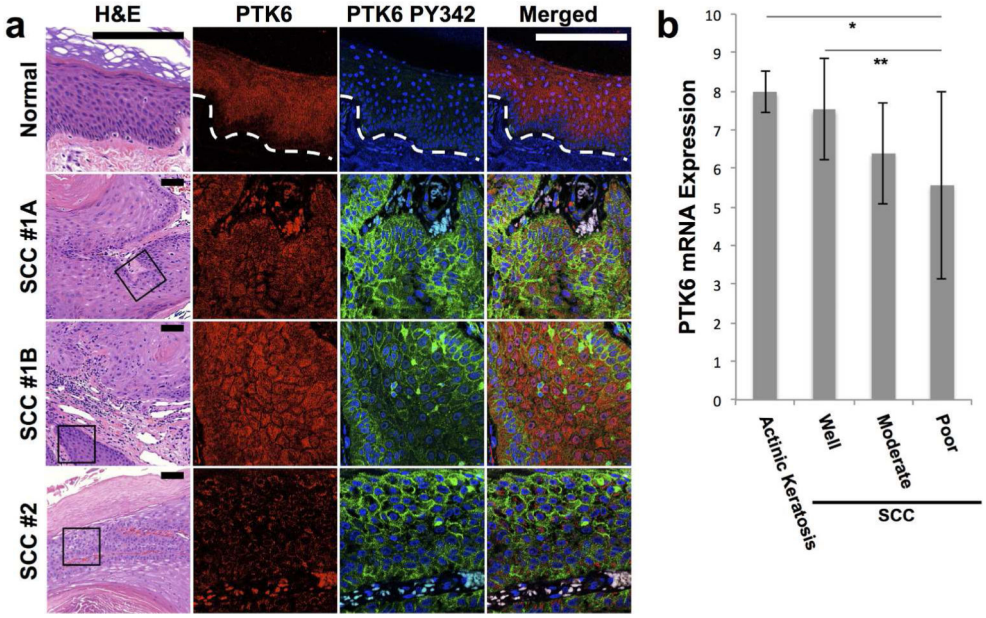

Figure 6. PTK6 is activated and membrane associated in human SCC

A: Expression of PTK6 in normal skin and SCC. Sections of human skin (normal, SCC) were costained for total PTK6 (Alexafluor 594, red) and active PY342 PTK6 (FITC, green) as described. A lower magnification H&E view with the area of interest boxed is also shown. Total PTK6 expression is restricted to the suprabasal layers of normal human skin. Little active PTK6 PY342 is present in the normal skin; a rare positive basal cell may be a lymphocyte. PTK6 is phosphorylated at the membrane of the basal layer in human squamous cell carcinoma samples. In SCC, highest levels of total PTK6 are expressed in suprabasal areas, while active membrane associated PTK6 is in the basal cell-like regions. Staining from two areas from the same patient sample, SCC1A and SCC1B are shown, while SCC#2 is from a different patient. 18 SCC samples were analyzed. Fluorescent signals over the red blood cells is background, that can also be detected with control IgG (not shown). Size bar = 20 μm. **B:** Transcriptome analysis of RNA expression in squamous cell carcinoma (Lambert *et al*., 2014) revealed PTK6 mRNA expression decreases in squamous cell carcinomas compared with actinic keratosis (p-value* = 0.008). The drop in PTK6 mRNA expression in squamous cell carcinomas corresponds with decreased differentiation (p-value** = 0.031).